5290 *Chem. Mater.* **2010,** *22,* 5290–5295
DOI:10.1021/cm101441p

CHEMISTRY OF MATERIALS
Article

Theoretical Investigation of the Magnetic Structure and Ferroelectric Polarization of the Multiferroic Langasite $Ba_3NbFe_3Si_2O_{14}$

Changhoon Lee,[†] Erjun Kan,[†] Hongjun Xiang,[‡] and Myung-Hwan Whangbo*,[†]

[†]*Department of Chemistry, North Carolina State University, Raleigh, North Carolina 27695, and* [‡]*Key Laboratory of Computational Physical Sciences, Ministry of Education, and Department of Physics, Fudan University, Shanghai 200433, P. R. China*

Received May 22, 2010. Revised Manuscript Received July 26, 2010

The multiferroic langasite $Ba_3NbFe_3Si_2O_{14}$, crystallizing in a noncentrosymetric space group, has sheets of Fe^{3+} ions parallel to the *ab* plane. It adopts a chiral magnetic order below $T_N = 26$ K that has a superstructure with propagation vector (0, 0, ~1/7). The spin frustration causing this magnetic structure of $Ba_3NbFe_3Si_2O_{14}$ was examined by evaluating its spin exchange interactions on the basis of density functional calculations and also by calculating its magnetic dipole−dipole interactions. The contribution of the chiral magnetic structure to the ferroelectric polarization of $Ba_3NbFe_3Si_2O_{14}$ below T_N was estimated by Berry phase calculations. The spin exchanges of $Ba_3NbFe_3Si_2O_{14}$ are frustrated in each //*ab* sheet and between adjacent sheets of Fe^{3+} ions. The helical spin rotation along the *c* axis occurs to minimize the intersheet spin frustration as well as the intersheet magnetic dipole−dipole interactions. The ferroelectric polarization of $Ba_3NbFe_3Si_2O_{14}$ estimated from calculations is in good agreement with the experimental value.

1. Introduction

The langasite $Ba_3NbFe_3Si_2O_{14}$, crystallizing in a nonsentrosymmetric space group $P321$,[1,2] is a spin-frustrated antiferromagnet with Curie−Weiss temperature $\theta = -190$ K and Néel temperature $T_N = 26$ K,[2] and exhibits a ferroelectric (FE) polarization below T_N.[2] In this compound each NbO_6 octahedron shares its corners with six FeO_4 tetrahedra to form a Fe_6 trigonal prism (Figure 1a) such that the FeO_4 and NbO_6 polyhedra make the "$NbFe_3O_{12}$" chains running along the *c* axis (Figure 1b). When linked by SiO_4 tetrahedra by corner sharing, these chains lead to the $NbFe_3Si_2O_{14}$ framework with pockets for the Ba^{2+} ions (Figure 1c). Among the Fe^{3+} (d^5), Nb^{5+} (d^0), Si^{4+}, and Ba^{2+} ions, the only magnetic ions are the Fe^{3+} ions that exist in the high-spin state ($S = 5/2$).[3] The Fe^{3+} ions form sheets of isolated Fe^{3+} triangles parallel to the *ab* plane (hereafter, the //*ab* sheets) (Figure 2a). Below T_N, the Fe^{3+} magnetic moments adopt a triangular 120° configuration within each Fe^{3+} triangle, which propagates in-phase within each triangular plane of Fe^{3+} ions but is helically modulated from one //*ab* sheet to another with a propagation vector (0, 0, ~1/7).[3] Thus, along every chain of Fe^{3+} ions parallel to the *c* axis, each Fe^{3+} magnetic moment rotates around the chain by the helical rotational angle ϕ of ~51° from one //*ab* sheet to another. [For convenience, this chiral magnetic structure will be referred to as the 120°/($\phi \approx 51°$) magnetic structure.] Consequently, the Fe^{3+} moments have a noncollinear arrangement within each //*ab* sheet and between adjacent //*ab* sheets, so that the spin exchanges between the Fe^{3+} ions are frustrated[4,5] not only within each //*ab* sheet but also between adjacent //*ab* sheets. Furthermore, the helical rotation of the Fe^{3+} moments leading to the (0, 0, ~1/7) superstructure indicates that the intersheet spin exchanges should obey a specific relationship because a noncollinear spin arrangement occurs to minimize the extent of spin frustration.[4,5] It is important to explore this relationship, for which one needs to evaluate the spin exchange interactions of $Ba_3NbFe_3Si_2O_{14}$.

For a crystalline solid to exhibit FE polarization, it should not possess inversion symmetry.[6,7] A centrosymmetric magnetic solid can lose inversion symmetry either by cooperative second-order Jahn−Teller distortion or by chiral magnetic order.[6−8] In principle, a noncentrosymmetric magnetic solid can have FE polarization independent of its magnetic structure. By analogy with the spin-frustrated multiferroic

*Corresponding author. E-mail: mike_whangbo@ncsu.edu.

(1) Marty, K.; Simonet, V.; Ballou, E. R.; Lejay, P.; Bordet, P. *Phys. Rev. Lett.* **2008**, *101*, 247201.
(2) Zhou, H. D.; Lumata, L. L.; Kuhns, P. L.; Reyes, A. P.; Choi, E. S.; Dalal, N. S.; Lu, J.; Jo, Y. J.; Balicas, L.; Brooks, J. S.; Wiebe, C. R. *Chem. Mater.* **2009**, *21*, 156.
(3) Marty, K.; Simonet, V.; Ballou, E. R.; Lejay, P.; Bordet, P.; Isnard, O.; Ressouche, E.; Bourdarot, F.; Bonville, P. *J. Magn. Magn. Mater.* **2009**, *321*, 1778.
(4) Greedan, J. E. *J. Mater. Chem.* **2001**, *11*, 37.
(5) Dai, D.; Whangbo, M.-H. J. *Chem. Phys.* **2004**, *121*, 672.
(6) (a) Ramesh, R.; Spaldin, N. A. *Nat. Mater.* **2007**, *6*, 21. (b) Khomskii, D. *Physics* **2009**, *2*, 20.
(7) (a) Eerenstein, W.; Mathur, N. D.; Scott, J. F. *Nature* (*London*) **2006**, *442*, 759. (b) Cheong, S. W.; Mostovoy, M. *Nat. Mater.* **2007**, *6*, 13. (c) Tokura, Y. *J. Mag. Mag. Mater.* **2007**, *310*, 1145.
(8) Kan, E. J.; Xiang, H. J.; Lee, C.; Wu, F.; Yang, J. L.; Whangbo, M.-H. *Angew. Chem., Int. Ed.* **2010**, *49*, 1603.

Published on Web 08/27/2010

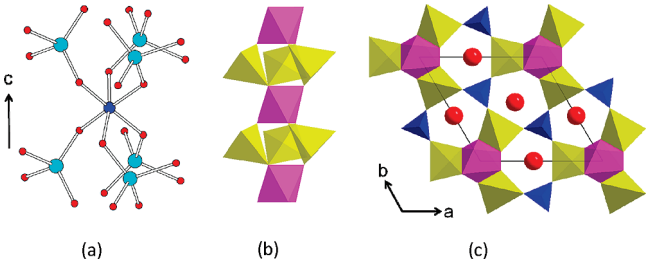

Figure 1. Structural features of $Ba_3NbFe_3Si_2O_{14}$: (a) Perspective view of an NbO_6 octahedron sharing corners with six FeO_4 tetrahedra forming a Fe_6 trigonal prism, where the Fe, Nb, and O atoms are represented by cyan, blue, and red circles, respectively. (b) Polyhedral view of an $NbFe_3O_{12}$ chain made up of NbO_6 octahedra and FeO_4 tetrahedra. (c) Polyhedral view of $Ba_3NbFe_3Si_2O_{14}$ projected along the c direction, where the NbO_6, FeO_4 and SiO_4 polyhedra are represented by the purple, beige, and blue polyhedra, respectively. The red spheres represent the Ba^{2+} cations.

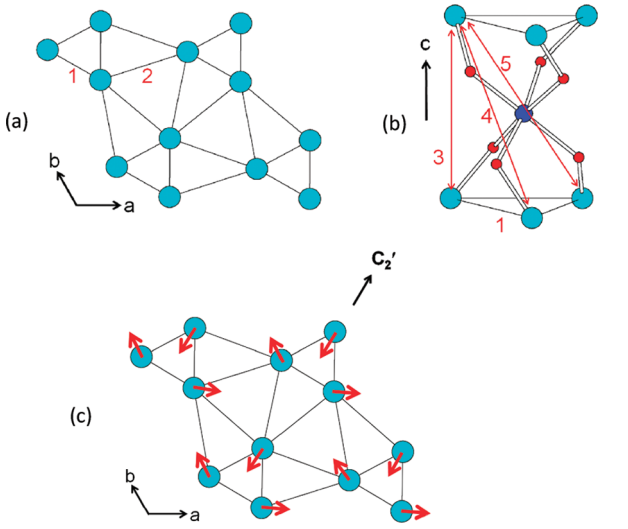

Figure 2. (a) Spin exchanges J_1 and J_2 of $Ba_3NbFe_3Si_2O_{14}$ (see Table 1) within each triangular plane of Fe^{3+} ions. (b) Spin exchanges J_3, J_4, and J_5 of $Ba_3NbFe_3Si_2O_{14}$ between adjacent triangular planes of Fe^{3+} ions. (c) Noncollinear spin arrangement in each //*ab* sheet of Fe^{3+} ions in $Ba_3NbFe_3Si_2O_{14}$ found in the magnetic structure below T_N.

$HoMnO_3$,[9] in which the displacement of Ho atoms along the c axis is responsible for its FE polarization, Zhou et al.[2] considered the possibility that the FE polarization of $Ba_3NbFe_3Si_2O_{14}$ arises from a bulking or tilting of the NbO_6 octahedra with some component along the c direction. However, the low temperature X-ray diffraction patterns of $Ba_3NbFe_3Si_2O_{14}$ showed neither structural phase transition nor structural distortion around T_N. Thus, it is crucial to see if the FE polarization of $Ba_3NbFe_3Si_2O_{14}$ observed below $T_N = 26$ K is caused by the ordered magnetic structure, because the latter is chiral and hence has no inversion symmetry.[3]

In the present work, we explore the aforementioned questions concerning the magnetic structure and FE polarization of $Ba_3NbFe_3Si_2O_{14}$ on the basis of density functional and magnetic dipole−dipole (MDD) energy calculations.[10,11] Results of our analyses are described in the following.

(9) Zhou, H. D.; Denyszyn, J. C.; Goodenough, J. B. *Phys. Rev. B* **2005**, *72*, 224401.
(10) Koo, H.-J.; Xiang, H. J.; Lee, C.; Whangbo, M.-H. *Inorg. Chem.* **2009**, *48*, 9051.
(11) Wu, F.; Kan, E. J.; Tian, C.; Whangbo, M.-H., *Inorg. Chem.*, submitted for publication.

Table 1. Geometrical Parameters Associated with the Spin Exchange Paths J_1−J_5 in $Ba_3NbFe_3Si_2O_{14}$

	Fe···Fe (Å)	O···O (Å)	bridge
J_1	3.762	2.747 (× 2)	O−Nb−O
J_2	5.668	2.210	O−Si−O
J_3	5.252	3.084	O−Nb−O
J_4	6.461	2.787	O−Nb−O
J_5	6.461	4.005	O−Nb−O

2. Computational Details

For the analysis of the magnetic structure of $Ba_3NbFe_3Si_2O_{14}$, we evaluate its spin exchanges defined in Figure 2 by performing mapping analysis based on density functional calculations. Our calculations employed the frozen-core projector augmented wave method encoded in the Vienna ab initio simulation packages,[12] and the generalized-gradient approximation (GGA)[13] with the plane-wave-cutoff energy of 400 eV and a set of 80 k points for the irreducible Brillouin zone. To examine the effect of electron correlation in the Fe 3d states, the GGA plus on-site repulsion method (GGA+U)[14] was used with the effective U values of 0, 3, and 5 eV. The FE polarization of $Ba_3NbFe_3Si_2O_{14}$ was determined by Berry phase calculations[15] on the basis of GGA+U plus spin−orbit coupling (SOC) interactions. The MDD interactions of $Ba_3NbFe_3Si_2O_{14}$ were calculated as a function of the helical rotation angle ϕ of the Fe^{3+} ion moments as described elsewhere.[10,11]

3. Spin Exchanges and Magnetic Structure

3.1. Extraction of Spin Exchange Parameters. As for the spin exchanges of $Ba_3NbFe_3Si_2O_{14}$, there are five Fe−O···O−Fe supersuperexchanges J_1−J_5 to consider. Within each //*ab* sheet of the Fe^{3+} ions (Figure 2a), J_1 is mediated by an O−Nb−O bridge, and J_2 by an O−Si−O bridge. Between adjacent //*ab* sheets of the Fe^{3+} ions, J_3−J_5 are mediated by O−Nb−O bridges (Figure 2b). To determine the values of these exchanges, we examine the five ordered spin states, defined in Figure 3 in terms of a (2a, b, 2c) supercell containing four formula units (FUs). The total spin exchange energies of these states, per FU, can be expressed in terms of the spin Hamiltonian $\hat{H} = -\sum_{i<j} J_{ij}\hat{S}_i \cdot \hat{S}_j$, where $J_{ij} = J_1$−J_5. By applying the energy expressions obtained for spin dimers with N unpaired spins per spin site (in the present case, $N = 5$),[16] the total spin exchange energies of the five ordered spin states, per FU, are written as

$$\begin{aligned} &\text{FM}: (-3J_1 - 6J_2 - 3J_3 - 3J_S)(N^2/4) \\ &\text{AF1}: (-3J_1 - 6J_2 + 3J_3 + 3J_S)(N^2/4) \\ &\text{AF2}: (+J_1 + 2J_2 - 3J_3 + J_S)(N^2/4) \\ &\text{AF3}: (+J_1 - 2J_2 - 3J_3 + J_S)(N^2/4) \\ &\text{AF4}: (+J_1 - 2J_2 + 3J_3 - J_S)(N^2/4) \end{aligned} \quad (1)$$

where $J_S = J_4 + J_5$. The exchanges J_4 and J_5 occur as a sum in the ordered spin states due to the trigonal symmetry of

(12) (a) Kresse, G.; Hafner, J. *Phys. Rev. B* **1993**, *47*, 558. (b) Kresse, G.; Furthmüller, J. *Comput. Mater. Sci.* **1996**, *6*, 15. (c) Kresse, G.; Furthmüller, J. *Phys. Rev. B* **1996**, *54*, 11169.
(13) Perdew, J. P.; Burke, K.; Ernzerhof, M. *Phys. Rev. Lett.* **1996**, *77*, 3865.
(14) Dudarev, S. L.; Botton, G. A.; Savrasov, S. Y.; Humphreys, C. J.; Sutton, A. P. *Phys. Rev. B* **1998**, *57*, 1505.
(15) King-Smith, R. D.; Vanderbilt, D. *Phys. Rev. B* **1993**, *47*, 1651. Resta, R. *Rev. Mod. Phys.* **1994**, *66*, 899.
(16) (a) Dai, D.; Whangbo, M.-H. *J. Chem. Phys.* **2001**, *114*, 2887. (b) Dai, D.; Whangbo, M.-H. *J. Chem. Phys.* **2003**, *118*, 29.

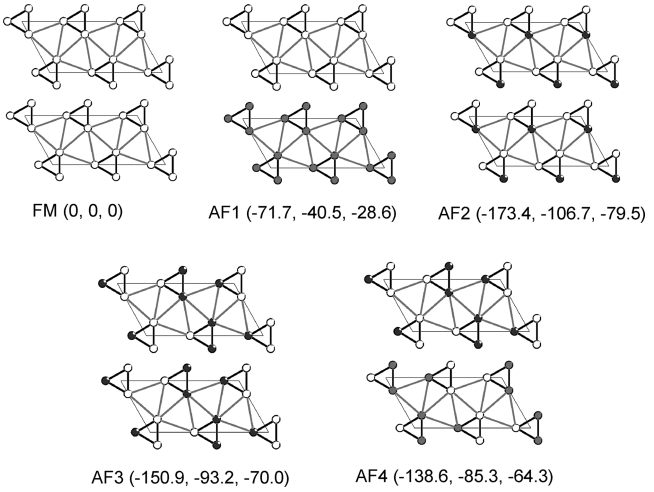

Figure 3. Five ordered spin states of $Ba_3NbFe_3Si_2O_{14}$ employed to extract the spin exchanges J_1, J_2, J_3, and $J_S = J_4 + J_5$. These states are defined by using a (2a, b, 2c) supercell, so that each spin state is specified by two parallelograms representing two (2a, b) cells parallel to the *ab* plane. The unshaded and shaded circles represent the Fe^{3+} ions with up-spin and down-spin, respectively. The three numbers in the parentheses (from left to right) for each state are the relative energies (per magnetic supercell, i.e., per 4 FUs) obtained from the GGA+U calculations (with U = 0, 3, and 5 eV, respectively).

$Ba_3NbFe_3Si_2O_{14}$, so that their values cannot be separated by mapping analysis. Therefore, we evaluate the four exchanges J_1, J_2, J_3, and J_S by employing the relative energies of the five ordered states from GGA+U calculations. These calculations show that all five states have a band gap even when $U = 0$, and the energy differences between the states become smaller with increasing U, as summarized in Figure 3. By mapping the relative energies of the five spin ordered states onto the corresponding energies expected from the total spin exchange energies listed in eq 1, we obtain the values of the exchanges summarized in Table 2.

To see how reasonable the calculated spin exchanges are, we calculate the Curie−Weiss temperature θ, which in the mean field theory[17] is related to spin exchange parameters as

$$\theta = \frac{S(S+1)}{3k_B}\sum_i z_i J_i \qquad (2)$$

where the summation runs over all nearest neighbors of a given spin site, z_i is the number of nearest neighbors connected by the spin exchange parameter J_i, and S is the spin quantum number of each spin site (i.e., $S = 5/2$ in the present case). Thus, for $Ba_3NbFe_3Si_2O_{14}$, θ can be approximated by

$$\theta \approx \frac{35(2J_1 + 4J_2 + 2J_3 + 2J_S)}{12k_B} \qquad (3)$$

The θ value is estimated to be −486, −296, and −220 K by using the spin exchange parameters from the GGA+U calculations with U = 0, 3, and 5 eV, respectively. Given the experimental θ value of −190 K, the spin exchange values are overestimated by a factor f = 2.55, 1.56, and 1.16 for U = 0, 3, and 5 eV, respectively. GGA+U electronic structure calculations generally overestimate the magnitude of spin exchange interactions by a factor approximately up to four.[18] Nevertheless, the relative values of the calculated spin exchanges are nearly independent of the U value.

Table 2. Values of the Spin Exchange Parameters in k_BK of $Ba_3NbFe_3Si_2O_{14}$ obtained from GGA+U calculations as a function of U[a]

	U = 0 eV	U = 3 eV	U = 5 eV
J_1	−40.1 (1.00)	−25.7 (1.00)	−20.1 (1.00)
J_2	−10.5 (0.26)	−6.3 (0.25)	−4.4 (0.22)
J_3	−2.7 (0.07)	−1.3 (0.05)	−0.9 (0.04)
J_S	−19.5 (0.49)	−11.2 (0.44)	−8.0 (0.40)

[a] The numbers in parentheses are the relative values.

3.2. Spin Frustration and Helical Spin Rotation. Table 2 shows that all Fe−O···O−Fe spin exchanges are antiferromagnetic, and the strongest spin exchange is the intrasheet exchange J_1. Within each //*ab* sheet of Fe^{3+} ions, J_1 is more strongly antiferromagnetic than J_2 by a factor of about 4. This means that the Fe−O···O−Fe exchange is more efficient through the O−Nb−O bridge than through the O−Si−O bridge, which arises from the fact that the bridge through a d^0 metal ion is more effective than that through a main-group cation.[19,20] As a consequence, the extent of spin frustration is much stronger in the (J_1, J_1, J_1) triangles than in the (J_2, J_2, J_2) triangles. Between adjacent //*ab* sheets of Fe^{3+} ions, the exchange J_3 is weak but J_S is strong (namely, $J_3/J_1 \approx 0.05$, and $J_S/J_1 \approx 0.45$). Because J_4 and J_5 are of a supersuperexchange type, both exchanges should be antiferromagnetic.[20] Then, the interlayer spin exchanges in the (J_1, J_3, J_4), (J_1, J_3, J_5) and (J_1, J_4, J_5) triangles are frustrated. To estimate the relative strengths of J_4 and J_5, we carried out spin dimer analysis[20] by performing extended Hückel tight binding calculations[20,21] for their associated spin dimer units (FeO_4)(NbO_4)(FeO_4). This analysis indicates that J_4 is substantially stronger than J_5 (i.e., $J_4/J_5 \approx 10$).

The spin exchange J_1 is considerably stronger than other exchanges, and the (J_1, J_1, J_1) triangles are spin frustrated, so that the pattern of the intrasheet spin arrangement (Figure 2c) is set by the compromised spin arrangement of the (J_1, J_1, J_1) triangles.[4,5] Perpendicular to such sheets, the spins rotate around the *c* axis forming a helix of period ∼7 lattice parameters. Because the intersheet spin exchanges are frustrated, the helical spin rotation around the *c* axis should be related to the intersheet spin frustration. To probe this point, we calculate the total intersheet spin exchange energy per spin site, $E_{SE}(\phi)$, for cases when the spins of one sheet is rotated around the *c* axis by ϕ with respect to those of its adjacent sheets.

(17) Smart, J. S. *Effective Field Theory of Magnetism*; Saunders: Philadelphia, 1966.

(18) (a) Xiang, H. J.; Lee, C.; Whangbo, M.-H. *Phys. Rev. B: Rapid Commun.* **2007**, *76*, 220411(R). (b) Koo, H.-J.; Whangbo, M.-H. *Inorg. Chem.* **2008**, *47*, 128. (c) Koo, H.-J.; Whangbo, M.-H. *Inorg. Chem.* **2008**, *47*, 4779.

(19) Dai, D.; Koo, H.-J.; Whangbo, M.-H. *Inorg. Chem.* **2004**, *43*, 4026. Koo, H.-J.; Whangbo, M.-H. *Inorg. Chem.* **2006**, *45*, 4440.

(20) Whangbo, M.-H.; Koo, H.-J.; Dai, D. *J. Solid State Chem.* **2003**, *417*, 176.

(21) Our calculations, carried out by using the CAESAR program package (http://chvamw.chem.ncsu.edu), show that $(\Delta e)^2$ = 860 and 80 $(meV)^2$ for J_4 and J_5, respectively, namely, $J_4/J_5 \approx 10$.

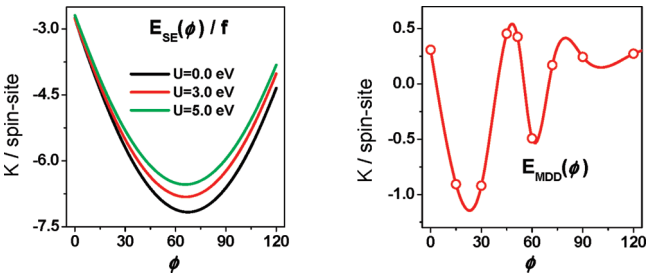

Figure 4. (a) Dependence on the helical rotation angle ϕ of the total intersheet spin exchange energy per spin site, $E_{SE}(\phi)/f$, where f is the factor by which the GGA+U calculations overestimate the calculated spin exchanges (i.e., $f = 2.55$, 1.56, and 1.16 for $U = 0$, 3, and 5 eV, respectively). (b) Dependence on the helical rotation angle ϕ of the total intersheet magnetic dipole−dipole interaction energy $E_{MDD}(\phi)$, where the solid curve, which is a guide for the eyes, is obtained from cubic spline fitting.

Because $S = 5/2$ for the high-spin Fe^{3+} ion, it is reasonable to treat the spin exchange interactions in terms of classical spin. Therefore, $E_{SE}(\phi)$ is written as

$$E_{SE}(\phi) = J_3 \cos\phi + J_S \cos(\phi + 120°) \quad (4)$$

The variation of $E_{SE}(\phi)$ as a function of ϕ in the region of $\phi = 0-120°$ is plotted in Figure 4a by using the J_3 and J_S values from the GGA+U calculations. The minimum of each $E_{SE}(\phi)$ vs ϕ curve occurs at the helical rotation angle ϕ_{min} satisfying the following condition

$$\tan\phi_{min} = \frac{(\sqrt{3}/2)J_S}{-J_3 + J_S/2} \quad (5)$$

from which we find $\phi_{min} = 67.4$, 66.1, and 65.7° for the sets of the J_3 and J_S from the GGA+U calculations with $U = 0$, 3, and 5 eV, respectively. These values are somewhat greater than the observed value $\phi_{obs} \approx 51.1°$. The ϕ_{min} value is determined largely by J_S, and the role of J_3 is to make ϕ_{min} greater than 60° (e.g., $\phi_{min} = 60°$ when $J_3 = 0$). This finding suggests that the discrepancy between ϕ_{min} and ϕ_{obs} is not caused by any inaccuracy of the calculated exchanges but rather by another energy factor affecting relative spin arrangements. This point is explored in the next section.

4. Magnetic Dipole−dipole Interactions and Helical Spin Rotation

The MDD interaction is a long-range interaction and is weak (of the order of ~0.1 meV for two spin-1/2 ions separated by 2 Å).[22] Though weak, this interaction is responsible for the occurrence of various ferromagnetic domains in a ferromagnet. These domains form because the overall MDD interaction energy is reduced by having domains with different spin directions. Therefore, we might consider if MDD interactions can decrease ϕ_{min} toward ϕ_{obs}. Our recent studies have shown that these interactions can play a crucial role in determining the 3D magnetic ordering and the spin orientation of magnetic solids based on 3d transition metals.[10,11] If we consider the spins as the classical spins, which is a good approximation for high-spin Fe^{3+} ($S = 5/2$) ions, the MDD interaction energy E_{MDD} of a given ordered spin arrangement is written as

$$EMDD = \sum_{i<j} \left(\frac{g^2\mu_B^2}{a_0^3}\right)\left(\frac{a_0}{r_{ij}}\right)^3 [-3(\vec{S}_i\vec{e}_{ij})(\vec{S}_j\vec{e}_{ij}) + (\vec{S}_i\vec{S}_j)] \quad (6)$$

where $\vec{S}_i$ and $\vec{S}_j$ are the spin vectors at the spin sites i and j, respectively, g is the electron g-factor, μ_B is the Bohr magneton, a_0 is the Bohr radius (0.529177 Å), r_{ij} is the distance between the spin sites i and j, and $\vec{e}_{ij}$ is the unit vector along the distance. Given that $(g\mu_B)^2/(a_0)^3 = 0.725$ meV, one can readily calculate E_{MDD} as a function of the helical rotation angle ϕ. In our calculations of the MDD interaction energy $E_{MDD}(\phi)$ as a function of the helical rotation angle ϕ, all MDD interaction terms are summed up with a cutoff radius of 450 Å, which is enough to make $E_{MDD}(\phi)$ converge. The calculated $E_{MDD}(\phi)$ vs ϕ plot is presented in Figure 4b in the range of $\phi = 0-120°$, which reveals that the $\phi = 0°$ spin arrangement is least stable, and there occur two minima, namely, a deep minimum around $\phi \approx 20$ and 60° with a sharp barrier between them. The minimum around $\phi \approx 60°$ is shallower than that around $\phi \approx 20°$, but will help decrease ϕ_{min} toward ϕ_{obs}, as anticipated. Note from Figure 4 that the energetic effect of the spin frustration is substantially stronger than that of the MDD interactions.

5. Ferroelectric Polarization of Noncentrosymmetric Solids

5.1. Dependence of Ferroelectric Polarization on Electric Field and Its Implication. Experimentally, the FE polarization P of a ferroelectric induced by magnetic order below its ordering temperature T_p is a relative value (i.e., the electric polarization below T_p minus that above T_p), and reverses its sign when the applied electric field E is reversed in direction. Let us first consider a multiferroic that has a centrosymmetric structure above T_p. The P vs E plot determined well below T_p shows a hysteresis loop due most likely to the presence of domains with different polarization directions. The reversal of the sign of P, which occurs below T_p when the sign of E is reversed, is often explained in terms of a double-well potential energy curve (Figure 5) for the structural transformation from one noncentrosymmetric structure with one FE polarization through a centrosymmetric structure with paraelectric (PE) polarization to an alternative noncentrosymmetric structure with opposite FE polarization. As schematically shown in Figure 5, the two FE structures of opposite FE polarizations are interconverted to each other through the PE structure.[23] It should be noted that any isolated structure, being a local-minimum-energy structure, cannot represent the PE structure because the

(22) Ashcroft, N. W.; Mermin, N. D. *Solid State Physics*; Saunders College: Philadelphia; 1976, pp 673−674.

(23) (a) Toupet, H.; Le Marrec, F.; Lichtensteiger, C.; Dkhil, B.; Karkut, M. G. *Phys. Rev. B* **2010**, *81*, 140101. (b) Arnold, D. C.; Knight, K. S.; Morrison, F. D.; Lightfoot, P. *Phys. Rev. Lett.* **2009**, *102*, 027602. (c) Selbach, S. M.; Tybell, T.; Einarsrud, M.-A.; Grande, T. *Adv. Mater.* **2008**, *20*, 3692. (d) Palai, R.; Katiyar, R. S.; Schmid, H.; Tissot, P.; Clark, S. J.; Robertson, J.; Redfern, S. A. T.; Catalan, G.; Scott, J. F. *Phys. Rev. B* **2008**, *77*, 014110. (e) Scott, J. F.; Palai, R.; Kumar, A.; Singh, M. K.; Murari, N. M.; Karan, N. K.; Katiyar, R. S. *J. Am. Chem. Soc.* **2008**, *91*, 1762.

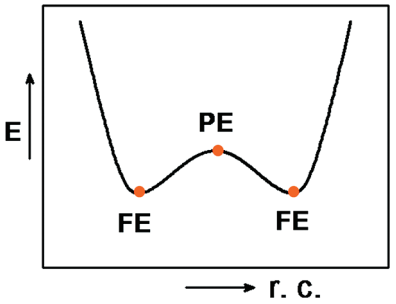

Figure 5. Schematic symmetric double-well potential energy curve for a ferroelectric system showing the interconversion between the two noncentrosymmetic FE structures with opposite FE polarizations through the centrosymmetric PE structure.

latter represents the transition state of the potential energy curve. It is commonly assumed that the interconversion between the two FE structures is achieved by applied electric field. This assumption is valid only when the energy barrier for the interconversion is small (Figure 5).

In explaining the field-induced polarization reversal of a multiferroic such as $Ba_3NbFe_3Si_2O_{14}$ that has a noncentrosymmetric structure above and below T_p, the aforementioned assumption is not valid. The crystal structure of $Ba_3NbFe_3Si_2O_{14}$ is chiral above and below T_p, and so is its ordered magnetic structure below T_p. As reported by Zhou et al.,[2] there is no structural evidence for the involvement of the NbO_6 octahedra in causing the FE polarization of $Ba_3NbFe_3Si_2O_{14}$. To reverse its FE polarization below T_p, therefore, either the crystal structure or the ordered magnetic structure of $Ba_3NbFe_3Si_2O_{14}$ must change its chirality. In general, there is no simple geometrical change that converts one chiral structure to its alternative chiral form, except for breaking all bonds and reassembling them. Therefore, the field-induced polarization reversal of $Ba_3NbFe_3Si_2O_{14}$ means that reversing the field direction modifies the ordered magnetic structure without altering a given chiral crystal structure. For energetic reasons, reversing the field direction must be accompanied by the reversal of FE polarization, which requires charge redistribution. The charge redistribution in an ordered magnetic state is governed by SOC interactions[24] and is hence affected by the nature of the ordered magnetic structure. In short, a chiral crystal structure with a chiral magnetic structure can have field-induced polarization reversal by changing the nature of the magnetic structure.

5.2. Estimation of the Ferroelectric Polarization of $Ba_3NbFe_3Si_2O_{14}$. A noncentrosymmetric system such as $Ba_3NbFe_3Si_2O_{14}$ should possess FE polarization not only below T_p, where it has a chiral magnetic structure, but also above T_p, where it has no long-range magnetic order. Thus, it is not straightforward how to estimate the FE polarization of such a system above T_p, because it has no PE structure and no long-range magnetic order. We calculate the FE polarization of $Ba_3NbFe_3Si_2O_{14}$ below T_N by using the Berry phase method[9] on the basis of GGA+U+SOC calculations for the commensurate magnetic state, i.e., the 120°/(ϕ = 51.43°) state, of $Ba_3NbFe_3Si_2O_{14}$. To simulate the FE polarization of $Ba_3NbFe_3Si_2O_{14}$ above T_N using this method, one might use an ordered magnetic state that would have inversion symmetry if the underlying atomic structure had no chirality. For this purpose, we employ the 120°/(ϕ = 0°) state, i.e., the state in which the helical rotational angle ϕ is reduced to 0°. In our GGA+U+SOC (with U = 3 eV) calculations for the 120°/(ϕ = 0°) state, the (a, b, 7c) supercell was used as in the case for the 120°/(ϕ = 51.43°) state. The overall pattern of the spin arrangement has a C_2' symmetry (i.e., C_2 rotation plus time reversal symmetry) along the (a+b) direction in both magnetic states, so the FE polarization P of $Ba_3NbFe_3Si_2O_{14}$ should be along the (a+b) direction,[25] and this is indeed the case from our calculations (see below). As summarized in Table 3, the FE polarizations of the 120°/(ϕ = 51.43°) and 120°/(ϕ = 0°) states are 12.9 and 2.4 $\mu C/m^2$, respectively, so that the difference between the FE polarizations of the two states is 10.5 $\mu C/m^2$. The latter is in reasonable agreement with the experimental value of ~9 $\mu C/m^2$.[2]

Table 3. Values of the FE Polarizations P (in $\mu C/m^2$) Calculated for the 120°/(ϕ = 51.43°) and 120°/(ϕ = 0°) States of $Ba_3NbFe_3Si_2O_{14}$ Obtained from GGA+U+SOC and GGA+U Calculations with U = 3 eV

	120°/(ϕ = 51.43°)	120°/(ϕ = 0°)
GGA+U+SOC	12.9	2.4
GGA+U	1.64	0.69

The FE polarization is negligible for both the 120°/(ϕ = 51.43°) and 120°/(ϕ = 0°) states from our GGA+U calculations. Therefore, SOC is essential for $Ba_3NbFe_3Si_2O_{14}$ to have FE polarization although it crystallizes in a noncentrosymmetric space group, as found for other magnetic-order-driven multiferroics whose space group is noncentrosymmetric above the magnetic ordering temperature.[24] This shows that the relaxed charge distribution appropriate for the noncentrosymmetric state reached by the magnetic order is obtained only when SOC interactions are taken into consideration.

Finally, we note that the energy $E(\phi)$ of $Ba_3NbFe_3Si_2O_{14}$ as a function of the helical rotation angle ϕ cannot be represented by a symmetrical double-well potential curve (e.g., Figure 5). Because J_4 and J_5 are considerably different, the helical rotation in one sense should be energetically more favorable than that in the opposite sense. It is important to find how the reversal of the electric field direction modifies the ordered magnetic structure and hence changes the sign of the ferroelectric polarization.

6. Concluding Remarks

The spin exchanges of $Ba_3NbFe_3Si_2O_{14}$ are frustrated in each //ab sheet and between adjacent sheets of Fe^{3+} ions. The intrasheet spin arrangement is set by the

(24) (a) Xiang, H. J.; Whangbo, M.-H. *Phys. Rev. Lett.* **2007**, *99*, 257203. (b) Xiang, H. J.; Wei, S.-H.; Whangbo, M.-H.; Da Silva, J. L. F *Phys. Rev. Lett.* **2008**, *101*, 037209. (c) Tian, C.; Lee, C.; Xiang, H. J.; Zhang, Y.; Payen, C.; Jobic, S.; Whangbo, M.-H. *Phys. Rev. B* **2009**, *80*, 104426.

(25) (a) Kan, E. J.; Xiang, H. J.; Zhang, Y.; Lee, C.; Whangbo, M.-H. *Phys. Rev. B* **2009**, *80*, 104417. (b) Seki, S.; Onose, Y.; Tokura, Y. *Phys. Rev. Lett.* **2008**, *101*, 067204. (c) Arima, T. *J. Phys. Soc. Jpn.* **2007**, *76*, 073702.

compromised spin arrangement of the (J_1, J_1, J_1) triangles. The helical spin rotation along the *c* axis occurs to minimize the intersheet spin frustration as well as the intersheet MDD interactions. By using the ($120°/\phi = 51.43°$) and ($120°/\phi = 0°$) states for Berry phase calculations, the FE polarization of $Ba_3NbFe_3Si_2O_{14}$ is estimated to change by $\sim 10.5\ \mu C/m^2$ along the ($a+b$) direction as it undergoes a magnetic ordering below T_N, which is in reasonable agreement with the experimental value of $\sim 9\ \mu C/m^2$. For the noncentrosymmetric state brought about by a chiral magnetic order to readjust its charge distribution, SOC interactions are essential. Currently we investigate what kinds of changes the reversal of the applied electric field direction must introduce in the ordered magnetic structure to cause the reversal of the electric polarization in $Ba_3NbFe_3Si_2O_{14}$

Acknowledgment. Work at NCSU was supported by the Office of Basic Energy Sciences, Division of Materials Sciences, U.S. Department of Energy, under Grant DE-FG02-86ER45259, and also by the computing resources of the NERSC center and the HPC center of NCSU.